



**HAL**  
open science

## **Electrochemical advanced oxidation processes using novel electrode materials for mineralization and biodegradability enhancement of nanofiltration concentrate of landfill leachates**

Marwa El Kateb, Clément Trelu, Alaa Darwich, Matthieu Rivallin, Mikhael Bechelany, Sakthivel Nagarajan, Stella Lacour, Nizar Bellakhal, Geoffroy Lesage, Marc Heran, et al.

► **To cite this version:**

Marwa El Kateb, Clément Trelu, Alaa Darwich, Matthieu Rivallin, Mikhael Bechelany, et al.. Electrochemical advanced oxidation processes using novel electrode materials for mineralization and biodegradability enhancement of nanofiltration concentrate of landfill leachates. *Water Research*, 2019, 162, pp.446-455. 10.1016/j.watres.2019.07.005 . hal-02278696

**HAL Id: hal-02278696**

**<https://hal.umontpellier.fr/hal-02278696v1>**

Submitted on 25 Oct 2021

**HAL** is a multi-disciplinary open access archive for the deposit and dissemination of scientific research documents, whether they are published or not. The documents may come from teaching and research institutions in France or abroad, or from public or private research centers.

L'archive ouverte pluridisciplinaire **HAL**, est destinée au dépôt et à la diffusion de documents scientifiques de niveau recherche, publiés ou non, émanant des établissements d'enseignement et de recherche français ou étrangers, des laboratoires publics ou privés.



Distributed under a Creative Commons Attribution - NonCommercial 4.0 International License

**Electrochemical advanced oxidation processes using novel electrode materials for mineralization and biodegradability enhancement of nanofiltration concentrate of landfill leachates.**

Marwa El Kateb<sup>1,2,4</sup>, Clément Trellu<sup>1,3,\*</sup>, Alaa Darwich<sup>1</sup>, Matthieu Rivallin<sup>1</sup>, Mikhael Bechelany<sup>1</sup>, Sakthivel Nagarajan<sup>1</sup>, Stella Lacour<sup>1</sup>, Nizar Bellakhal<sup>4</sup>, Geoffroy Lesage<sup>1</sup>, Marc Héran<sup>1</sup>, Marc Cretin<sup>1,\*</sup>

<sup>1</sup> IEM, Univ Montpellier, CNRS, ENSCM, Montpellier, France

<sup>2</sup> Université de Tunis El Manar, Faculté des Sciences de Tunis, 2092 Tunis, Tunisie

<sup>3</sup> Laboratoire Géomatériaux et Environnement, LGE – Université Paris-Est, EA 4508, UPEM,  
77454 Marne-la-Vallée, France

<sup>4</sup> Université de Carthage, Institut National des Sciences Appliquées et de Technologie,  
Laboratoire d’Echo-Chimie, 1080 Tunis, Tunisie

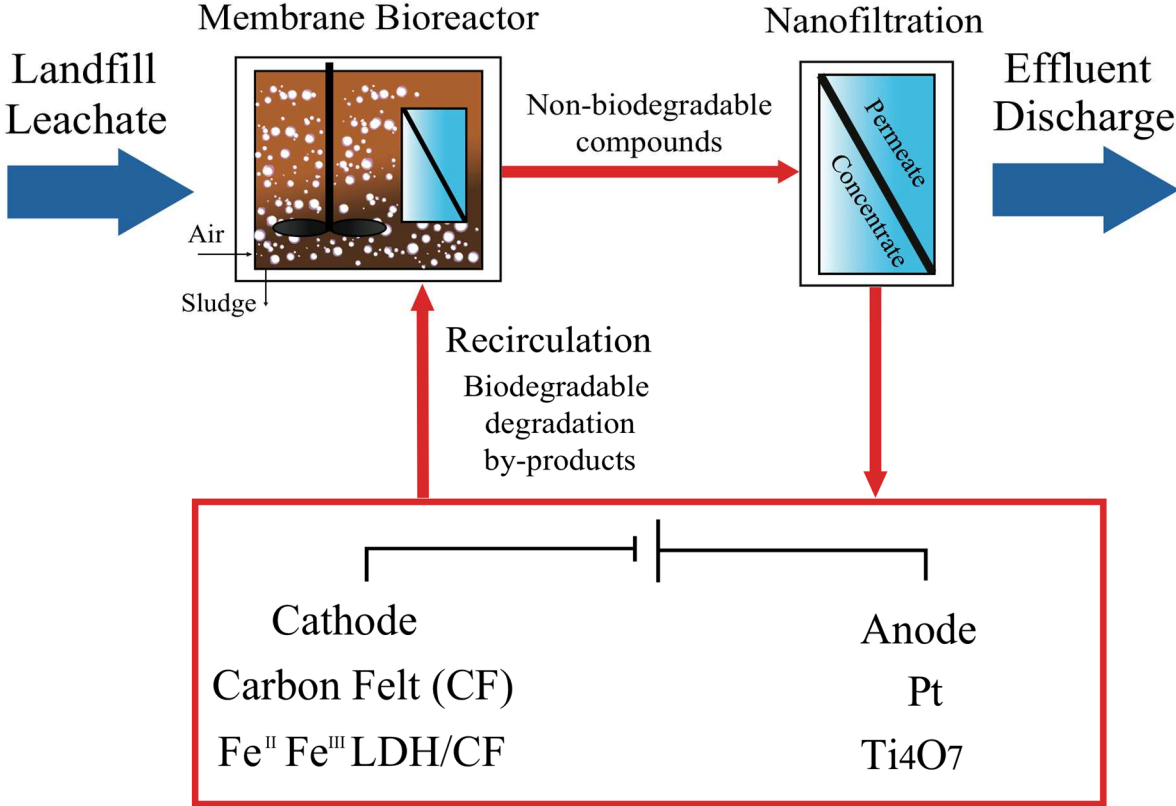
**Manuscript submitted to Water Research for consideration**

\* Corresponding Author:

clement.trellu@u-pem.fr

+33 1 49 32 90 42

**Graphical abstract**



**Electrochemical Advanced Oxidation Processes**  
**Homogeneous/Heterogeneous electro-Fenton**  
**Anodic Oxidation**

## 1 **Abstract**

2 The objective of this study was to implement electrochemical advanced oxidation processes  
3 (EAOPs) for mineralization and biodegradability enhancement of nanofiltration (NF)  
4 concentrate from landfill leachate initially pre-treated in a membrane bioreactor (MBR). Raw  
5 carbon felt (CF) or Fe<sup>II</sup>Fe<sup>III</sup> layered double hydroxides-modified CF were used for comparing  
6 the efficiency of homogeneous and heterogeneous electro-Fenton (EF), respectively. The  
7 highest mineralization rate was obtained by heterogeneous EF: 96% removal of dissolved  
8 organic carbon (DOC) was achieved after 8 h of electrolysis at circumneutral initial pH (pH<sub>0</sub>  
9 = 7.9) and at 8.3 mA cm<sup>-2</sup>. However, the most efficient treatment strategy appeared to be  
10 heterogeneous EF at 4.2 mA cm<sup>-2</sup> combined with anodic oxidation using Ti<sub>4</sub>O<sub>7</sub> anode (energy  
11 consumption = 0.11 kWh g<sup>-1</sup> of DOC removed). Respirometric analyses under similar  
12 conditions than in the real MBR emphasized the possibility to recirculate the NF retentate  
13 towards the MBR after partial mineralization by EAOPs in order to remove the residual  
14 biodegradable by-products and improve the global cost effectiveness of the process. Further  
15 analyses were also performed in order to better understand the fate of organic and inorganic  
16 species during the treatment, including acute toxicity tests (Microtox<sup>®</sup>), characterization of  
17 dissolved organic matter by three-dimensional fluorescence spectroscopy, evolution of  
18 inorganic ions (ClO<sub>3</sub><sup>-</sup>, NH<sub>4</sub><sup>+</sup> and NO<sub>3</sub><sup>-</sup>) and identification/quantification of degradation by-  
19 products such as carboxylic acids. The obtained results emphasized the interdependence  
20 between the MBR process and EAOPs in a combined treatment strategy. Improving the  
21 retention in the MBR of colloidal proteins would improve the effectiveness of EAOPs  
22 because such compounds were identified as the most refractory. Enhanced nitrification would  
23 be also required in the MBR because of the release of NH<sub>4</sub><sup>+</sup> from mineralization of refractory  
24 organic nitrogen during EAOPs.

25 **Keywords**

26 Electro-Fenton; Anodic oxidation; Modified carbon felt; Sub-stoichiometric titanium oxide;

27 Landfill leachate; Biodegradability.

## 28 **1. Introduction**

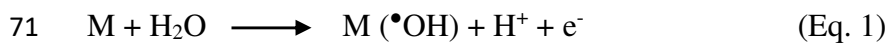
29 Rainwater percolation through waste layers of landfills generates leachates containing a  
30 complex mixture of dissolved organic matter (DOM), inorganic compounds, heavy metals,  
31 and xenobiotic organic substances (Kjeldsen et al., 2002), which represents a significant  
32 hazard for the environment.

33 The implementation of a membrane bioreactor (MBR) followed by a nanofiltration (NF) step  
34 is one of the most efficient treatment strategy currently used for management of landfill  
35 leachates (Campagna et al., 2013; Amaral et al., 2016). However, NF is only a separation  
36 process. Biorefractory organic pollutants are accumulated and concentrated. Thus, the  
37 concentrate becomes an important residual issue for this treatment strategy (Van der Bruggen  
38 et al., 2003; Zhang et al., 2009, 2013). Landfill discharge of the concentrate is commonly  
39 performed. However, some national regulations do not allow such practice and it clearly does  
40 not fix the long-term issue. In recent years, several processes have been investigated and  
41 applied at industrial scale for the treatment of NF concentrate. For example, adsorption  
42 processes are effective to remove organic matters in NF concentrate, but they are strongly  
43 limited by the high organic charge of such effluents compared to the adsorption capacity of  
44 adsorbent materials. Besides, membrane distillation and evaporation processes are  
45 substantially limited by the high cost of equipment and energy consumption (Cui et al., 2018).

46 During the last two decades, electrochemical advanced oxidation processes (EAOPs) have  
47 received great attention for efficient degradation of a large range of hazardous and  
48 biorefractory organic compounds. They are based on *in situ* electrogeneration of hydroxyl  
49 radicals ( $\bullet\text{OH}$ ), a non-selective and powerful oxidizing agent ( $E^\circ(\bullet\text{OH}/\text{H}_2\text{O}) = 2.80 \text{ V vs SHE}$ )  
50 (Brillas et al., 2009; Comninellis et al., 2008; Martínez-Huitle et al., 2015; Panizza and  
51 Cerisola, 2009). EAOPs provide also several technical advantages such as high versatility,

52 easy operation, possibility for automation and low consumption of chemical reagents  
53 (Radjenovic and Sedlak, 2015; Sirés et al., 2014). However, complete mineralization of  
54 organic compounds requires high energy consumption. Therefore, the combination of EAOPs  
55 with biological processes is currently more and more investigated as a feasible option for  
56 improving the global cost-effectiveness of the process (Oller et al., 2011; Ganzenko et al.,  
57 2014, 2018; Trellu et al., 2016a; Olvera-Vargas et al., 2015). In order to achieve reliable  
58 conclusions, the accurate assessment of biodegradability enhancement by EAOPs requires the  
59 use of proper measurement tools such as respirometric methods (Reuschenbach et al., 2003).

60 Anodic oxidation (AO) and electro-Fenton (EF) are the most popularized EAOPs (Brillas et  
61 al., 2009; Panizza and Cerisola, 2009; Martínez-Huitle et al., 2015; Oturan et al., 2015). AO is  
62 based on the generation of hydroxyl radicals ( $\bullet\text{OH}$ ) via water oxidation at the surface of  
63 anodes (M) with high overvoltage for oxygen evolution reaction (Eq. 1) (Panizza and  
64 Cerisola, 2009; Trellu et al., 2017; Özcan et al., 2008), while  $\bullet\text{OH}$  are generated  
65 homogeneously in the bulk during the EF process through the Fenton's reaction (Eq. 2)  
66 (Brillas et al., 2009; Ma et al., 2016; Zhang et al., 2007).  $\text{H}_2\text{O}_2$  and iron (II) are continuously  
67 electrogenerated at the cathode by reduction of dissolved oxygen (Eq. 3) and iron (III)  
68 reduction (Eq. 4), respectively. External oxygen supply is required and an iron source must be  
69 either initially added at catalytic amount to the treated solution (homogeneous EF) or  
70 embedded onto suitable electrode materials (heterogeneous EF).



75 Homogeneous EF requires external iron source and acidic pH (*i.e.* pH 2.5 – 3.5) that prevents  
76 iron precipitation (Brillas et al., 2009). Besides, heterogeneous EF using for example pyrite  
77 (Ammar et al., 2015) or iron loaded sepiolite (Iglesias et al., 2013) as iron source has been  
78 developed in order to operate the process over a wide pH range (Ganiyu et al., 2018; Poza-  
79 Nogueiras et al., 2018). Innovative electrodes have been also synthesized and studied as both  
80 heterogeneous catalyst source and cathode materials (Zhang et al., 2012; Wang et al., 2013;  
81 García-Rodríguez et al., 2016; Ganiyu et al., 2017a). Particularly, the modification of raw  
82 carbon felt (CF) with CoFe or Fe<sup>II</sup>Fe<sup>III</sup>-layered double hydroxide (LDH) also led to an  
83 increase of the electroactive surface area, which in turn improved the generation of H<sub>2</sub>O<sub>2</sub> and  
84 the global efficiency of the heterogeneous EF process (Ganiyu et al., 2017a, 2018). However,  
85 to the best of our knowledge, none study focused on the application of such promising  
86 electrodes for the treatment of real wastewaters.

87 As regards to anode materials, sub-stoichiometric titanium oxides (especially Ti<sub>4</sub>O<sub>7</sub>) recently  
88 received great attention for application in wastewater treatment by AO (Guo et al., 2016;  
89 Ganiyu et al., 2016; Trelu et al., 2018b). Ti<sub>4</sub>O<sub>7</sub> anode is able to generate large amounts of  
90 physisorbed hydroxyl radicals (Ti<sub>4</sub>O<sub>7</sub>(•OH)) for the degradation and mineralization of organic  
91 contaminants. Besides, this material has the potential to become a low-cost anode compared  
92 to the well known boron-doped diamond anode (Ganiyu et al., 2017b; Trelu et al., 2018b).  
93 However, to the best of our knowledge, such anode material has also still not been applied for  
94 the treatment of real effluents.

95 The objective of this study was to investigate the application of these novel electrode  
96 materials for the treatment of a NF concentrate of landfill leachate initially pre-treated in a  
97 MBR, which represents an important challenge for environmental engineering. Various  
98 configurations (*i.e.* homogeneous EF, heterogeneous EF, heterogeneous EF/AO) and  
99 operating conditions were studied. The efficiency for mineralization of organic compounds



100 was compared. A particular attention was also given to the understanding of mineralization  
101 mechanisms by using various analytical tools: (i) DOM was characterized by three-  
102 dimensional excitation and emission matrix fluorescence (3DEEM), (ii) degradation by-  
103 products such as short-chain carboxylic acids were identified and quantified by ion-exclusion  
104 HPLC, and (iii) inorganic ions released during the mineralization process were identified and  
105 quantified by ion chromatography. Moreover, acute toxicity of the effluent was assessed by  
106 Microtox<sup>®</sup> analysis and the possibility to use such EAOPs as a pre-treatment before  
107 recirculation towards the MBR was assessed by using respirometric method under similar  
108 conditions than in the real industrial MBR. Finally, recommendations were given by taking  
109 into consideration the interdependence of MBR process and EAOP in a combined treatment  
110 strategy.

111

## 112 **2. Materials and methods**

### 113 **2.1 Chemicals**

114 For the preparation of Fe<sup>II</sup>Fe<sup>III</sup>-LDH modified CF, iron III nitrate nonahydrate Fe(NO<sub>3</sub>)<sub>3</sub>.9H<sub>2</sub>O  
115 (CAS 7782-61-8, 98% purity), iron II sulfate heptahydrate FeSO<sub>4</sub>.7H<sub>2</sub>O (CAS 7782-63-0,  
116 >99% purity), urea CO(NH<sub>2</sub>)<sub>2</sub> (CAS 57-13-6) and ammonium fluoride NH<sub>4</sub>F (CAS 12125-01-  
117 8, 99% purity) were supplied by Sigma Aldrich. Ultra-pure water (Millipore Mill-Q system,  
118 resistivity >18 MΩ.cm at 25 °C) was used for the preparation of all solutions.

119

### 120 **2.2 Landfill leachate (NF concentrate)**

121 The NF concentrate was collected from a landfill leachate wastewater treatment plant  
122 (WWTP) in the south of France. The raw landfill leachate was initially treated in a MBR, then

123 followed by a NF step. The concentrate from the NF step was collected and stored in a  
124 refrigerator at 4 °C.

125

### 126 **2.3 Electrochemical setup and electrode materials**

127 Experiments were conducted in an undivided cylindrical glass containing 220 mL of NF  
128 concentrate at room temperature (25 °C). The electrochemical cell was similar to the one used  
129 in several previous studies (Ganiyu et al., 2016; Trelu et al., 2016b). Either raw CF (for  
130 homogeneous EF) or Fe<sup>II</sup>Fe<sup>III</sup>-LDH modified CF (for heterogeneous EF) was employed as  
131 cathode (20 x 6 cm; 120 cm<sup>2</sup>), positioned on the inner wall of the cylindrical cell. CF (99.0%,  
132 6.35 mm thick) was provided by Alfa Aesar. Fe<sup>II</sup>Fe<sup>III</sup>-LDH modified CF was prepared by *in-*  
133 *situ* solvothermal process as reported elsewhere (Ganiyu et al., 2018). LDH coating was 0.62  
134 ± 0.04 mg cm<sup>-2</sup>, which was also in agreement with what has been reported previously (Ganiyu  
135 et al., 2018). For homogeneous EF experiments, 0.2 mM of Fe<sup>2+</sup> was added to the solution  
136 and initial pH was adjusted at 3 (values usually reported as optimal). For heterogeneous EF  
137 experiments, none Fe<sup>2+</sup> was externally added and pH was not initially adjusted.

138 The anode was either a 24 cm<sup>2</sup> (3 x 8 cm) platinum mesh (for homogeneous and  
139 heterogeneous EF) or a 32 cm<sup>2</sup> (4 x 8 cm) Ti<sub>4</sub>O<sub>7</sub> thin film plasma deposited on Ti substrate  
140 (for heterogeneous EF/AO) from Saint-Gobain Research Provence, France. Ti<sub>4</sub>O<sub>7</sub> powder  
141 used for plasma deposition was prepared by carbothermal reduction of TiO<sub>2</sub> as already  
142 reported by our group (Ganiyu et al., 2016, 2017b). These rectuganlar-shaped anodes were  
143 placed at the center of the cylindrical electrochemical cell, with an average interelectrode  
144 distance of 3 cm.

145 Electrodes were connected to a DC power supply (CNB Electronique) with applied current set  
146 at 1000 mA ( $j = 8.3 \text{ mA cm}^{-2}$ , calculated from the cathode surface, which is the working

147 electrode during the EF process) or 500 mA ( $j = 4.2 \text{ mA cm}^{-2}$ ). A magnetic stirrer was used to  
148 improve mass transport of chemical species toward/from the electrodes. The solution was  
149 saturated with  $\text{O}_2$  by bubbling compressed air through a glass frit 10 min before starting the  
150 experiments and all along the electrolysis. The conductivity of the NF concentrate was high  
151 enough to ensure the electrolysis without any additional supporting electrolyte. For  
152 comparison, a reference experiment was also carried out using raw carbon felt cathode, Pt  
153 anode, without adding any source of iron and without initial pH adjustment.

154

#### 155 **2.4 Dissolved organic carbon and chemical oxygen demand analysis**

156 Mineralization rate of NF concentrate was determined by total organic carbon (TOC) analyses  
157 using the Shimadzu TOC-L analyzer based on the 680 °C combustion catalytic oxidation  
158 method. All samples were filtrated through 0.45  $\mu\text{m}$  regenerated cellulose (RC) membrane  
159 filters. Therefore, results are reported as dissolved organic carbon (DOC).

160 Chemical oxygen demand (COD) was analyzed by the method AFNOR NFT 90-101 using  
161 Hach COD kits.

162

#### 163 **2.5 Respirometric method for the determination of biodegradability**

164 Biodegradability was assessed with a BM-T Advance Respirometer (SURCIS S.L, Spain),  
165 which consists in a 1 L capacity vessel, provided with an oxygen probe (Hamilton) and  
166 temperature control system. The activated sludge used in the bioassays was collected from the  
167 aerated tank of the landfill leachate WWTP using MBR and was thus acclimatized to the  
168 effluent. The samples were evaluated without pH adjustment because of the high buffer  
169 capacity of the landfill leachate samples. Continuous aeration and agitation were applied to

170 ensure air saturation conditions. Temperature was maintained at 20 °C during the tests and the  
171 standardization with sodium acetate method was applied (conversion rate adjustment  
172 according to instructions given by the respirometer's manufacturer). In order to inhibit the  
173 nitrification process and measure the sample effect only on the heterotrophic bacteria, 1.5 mg  
174 gVSS<sup>-1</sup> of N-allylthiourea was added before the beginning of each trial.

175 For biodegradability assays, 700 mL of endogenous activated sludge and 300 mL of target  
176 sample were introduced in the respirometer. The biodegradability of samples pre-treated by  
177 EAOPs was assessed through R tests (Fig. SI 1). The ratio between biodegradable COD  
178 (bCOD) and DOC (bCOD/DOC) was used for determination of the biodegradable character  
179 of each sample. A biodegradability enhancement index (BE) was calculated by using Eq. 5.

$$180 \quad BE = \frac{\left(\frac{bCOD_t}{DOC_t}\right)}{\left(\frac{bCOD_0}{DOC_0}\right)} \quad (\text{Eq. 5})$$

181 Where bCOD<sub>t</sub> and DOC<sub>t</sub> are bCOD (in gO<sub>2</sub> L<sup>-1</sup>) and DOC (in gC L<sup>-1</sup>) after t hours of  
182 treatment by EAOPs.

183

## 184 **2.6 Characterization of dissolved organic matter by three-dimensional excitation and** 185 **emission matrix fluorescence (3DEEM)**

186 Natural organic matter was characterized by 3DEEM fluorescence using a Perkin-Elmer LS-  
187 55 spectrometer (USA). The dilution factor was 200 for all samples. The procedure reported  
188 by Jacquin et al. (2017) was used for fluorescence spectra acquisition and data extraction.  
189 Chen et al. (2003) divided fluorescence spectra into five different areas corresponding to  
190 different groups of fluorophores, *i.e.* regions I and II for aromatic proteins, region III for  
191 fulvic acid-like (FA-like) fluorophores, region IV for soluble microbial by-product-like  
192 (SMP-like) fluorophores and region V for humic acid-like (HA-like) fluorophores (Chen et

193 al., 2003). Similarly to the study of Jacquin et al. (2017), 3DEEM results were analyzed by  
194 taking into consideration only 3 different zones, *i.e.* zone I' for region I + II (aromatic  
195 proteins), zone II' for region IV (SMP-like) and zone III' for region III + V (HA + FA-like).  
196 Calculation of the volume of fluorescence in these different zones was achieved following the  
197 method from Jacquin et al. (2017).

198

199 The procedures for ICP-MS analysis, toxicity test (Microtox<sup>®</sup>), identification/quantification of  
200 inorganic ions and identification/quantification of short-chain carboxylic acids are provided in  
201 Supplementary Information (SI)

202

## 203 **3. Results and Discussion**

### 204 **3.1 Characterization of the NF concentrate effluent**

205 The characteristics of the NF concentrate are presented in SI (Table SI 1). The effluent was a  
206 dark brown liquid having a slightly alkaline pH and high organic charge. The conductivity  
207 ( $3.1 \text{ mS cm}^{-1}$ ) was between 3 and 10 times lower than values reported in the literature ( $10 -$   
208  $33 \text{ mS.cm}^{-1}$ ) (Li et al., 2015; Hu et al., 2018; Xu et al., 2017). This might be ascribed to the  
209 high diversity of landfill leachate and to a lower retention of ionic species by the NF step. In  
210 fact, the concentration factor of divalent ( $\text{Mg}^{2+}$  and  $\text{Ca}^{2+}$ ) and monovalent ( $\text{Na}^+$  and  $\text{K}^+$ )  
211 inorganic cations was only  $3.1 \pm 0.3$  and  $1.7 \pm 0.2$ , respectively. Monovalent ions are less  
212 retained by the NF membrane because of lower charge interactions (Van der Bruggen et al.,  
213 2004). The COD content ( $2.1 \text{ gO}_2 \text{ L}^{-1}$ ) of the NF concentrate was also in the low range of  
214 values usually reported in the literature ( $1.7 - 5.5 \text{ gO}_2 \text{ L}^{-1}$ ) (Li et al., 2015; Hu et al., 2018; Xu

215 et al., 2017) because of (i) operation of the NF process with a lower concentration factor  
216 and/or (ii) lower initial organic loading rate of the effluent pre-treated by the MBR.

217 The ratio between bCOD and total COD or total DOC was low (bCOD/COD = 0.12 or  
218 bCOD/DOC = 0.26), thus indicating the low biodegradability of the concentrate owing to the  
219 presence of high-molecular weight and non-biodegradable compounds. A high concentration  
220 of nitrate ( $[\text{NO}_3^-] = 90 \text{ mg L}^{-1}$ ) was observed due to the complete nitrification of  $\text{NH}_4^+$  in the  
221 MBR and a partial denitrification in the anoxic tank. As regards to metals, Sr ion was the  
222 most concentrated ( $6.0 \text{ mg L}^{-1}$ ) and high concentrations of As ( $0.38 \text{ mg L}^{-1}$ ) and Cr ( $0.67 \text{ mg}$   
223  $\text{L}^{-1}$ ) ions were also reported. These metals are released by different wastes discarded in  
224 landfills such as glass products (Ponthieu et al., 2007), fluorescent lights and ceramics  
225 (Mahindrakar and Rathod, 2018). Besides, the high concentration of Sb ( $1.2 \text{ mg L}^{-1}$ ) indicates  
226 an important contamination from plastic decomposition (Westerhoff et al., 2008).

227

### 228 **3.2 Mineralization efficiency by EAOPs**

229 Various experiments were performed in order to evaluate the efficiency of different EAOPs  
230 (*i.e.* homogeneous EF, heterogeneous EF, heterogeneous EF/AO).

231 First, volatilization and adsorption phenomena were evidenced by bubbling oxygen into the  
232 electrochemical reactor without any current applied. Under these conditions, DOC content  
233 decreased and reached a plateau after 1 h with around  $16 \pm 2\%$  removal due to volatilization of  
234 volatile organic compounds and adsorption of hydrophobic compounds on CF. Besides, it was  
235 also observed that initial pH adjustment at 3 decreased the DOC value by  $15 \pm 5\%$  because of  
236 the precipitation of humic acids.

237 Second, experiments were carried out under constant current density applied to the electrodes.

238 As shown in Fig. 1A, 96% of DOC removal was obtained after 8 h of electrolysis by

239 heterogeneous EF with an applied current density of  $8.3 \text{ mA cm}^{-2}$ . The excellent  
240 mineralization efficiency achieved without any initial pH adjustment was ascribed to  
241 heterogeneous EF reaction occurring on the surface of the  $\text{Fe}^{\text{II}}\text{Fe}^{\text{III}}\text{-LDH}$  catalyst, which  
242 catalyzed the decomposition of  $\text{H}_2\text{O}_2$  to generate large amounts of hydroxyl radicals  $\bullet\text{OH}$   
243 (Ganiyu et al., 2018). By comparison, only 59% removal of DOC was obtained in the  
244 reference experiment with analogous operating conditions but using raw CF as cathode  
245 instead of  $\text{Fe}^{\text{II}}\text{Fe}^{\text{III}}\text{-LDH}$  modified CF, thus highlighting the benefits obtained from the use of  
246 the modified cathode. Heterogeneous EF was also even more efficient than conventional  
247 homogeneous EF (90% removal of DOC after 8 h) with external addition of iron catalyst ( $0.2$   
248  $\text{mmol L}^{-1}$ ) and initial adjustment of pH at 3. Therefore,  $\text{Fe}^{\text{II}}\text{Fe}^{\text{III}}\text{-LDH}$  modified CF appeared  
249 as an ideal cathode material that enhances the mineralization efficiency of the EF process and  
250 avoids both initial pH adjustment and external addition of iron. The stability and reusability of  
251 the prepared  $\text{Fe}^{\text{II}}\text{Fe}^{\text{III}}\text{-LDH}$  modified CF cathode was assessed by reusing the same electrode  
252 for 4 successive electrolysis cycles (Fig. 2). The slight but continuous decrease of the  
253 efficiency could be ascribed to (i) the initial loss of loosely bounded  $\text{Fe}^{\text{II}}\text{Fe}^{\text{III}}\text{-LDH}$  at the  
254 external surface of the CF substrate due to vigorous stirring and/or (ii) iron leaching at acidic  
255 pH for which  $\text{Fe}^{\text{II}}\text{Fe}^{\text{III}}\text{-LDH}$  coating is less stable. Indeed, a progressive reduction of pH to  
256 values in the range 3 - 4 was noticed during electrolysis, which was explained by the  
257 generation of short-chain carboxylic acids. This leaching phenomenon was confirmed by  
258 comparison of SEM images of raw CF,  $\text{Fe}^{\text{II}}\text{Fe}^{\text{III}}\text{-LDH}$  modified CF before use and  $\text{Fe}^{\text{II}}\text{Fe}^{\text{III}}\text{-}$   
259  $\text{LDH}$  modified CF after 4 cycles of electrolysis (Fig. SI 2). While an extensive growth on the  
260 CF of dense platelets of  $\text{Fe}^{\text{II}}\text{Fe}^{\text{III}}\text{-LDH}$  with uneven and porous structure was initially  
261 obtained, a partial degradation of the global  $\text{Fe}^{\text{II}}\text{Fe}^{\text{III}}\text{-LDH}$  structure was observed after 4  
262 cycles. Thus, in order to avoid the depletion of the catalyst, a continuous pH control

263 regulation would be recommended rather than a unique pH re-adjustment at the end of the  
264 treatment.

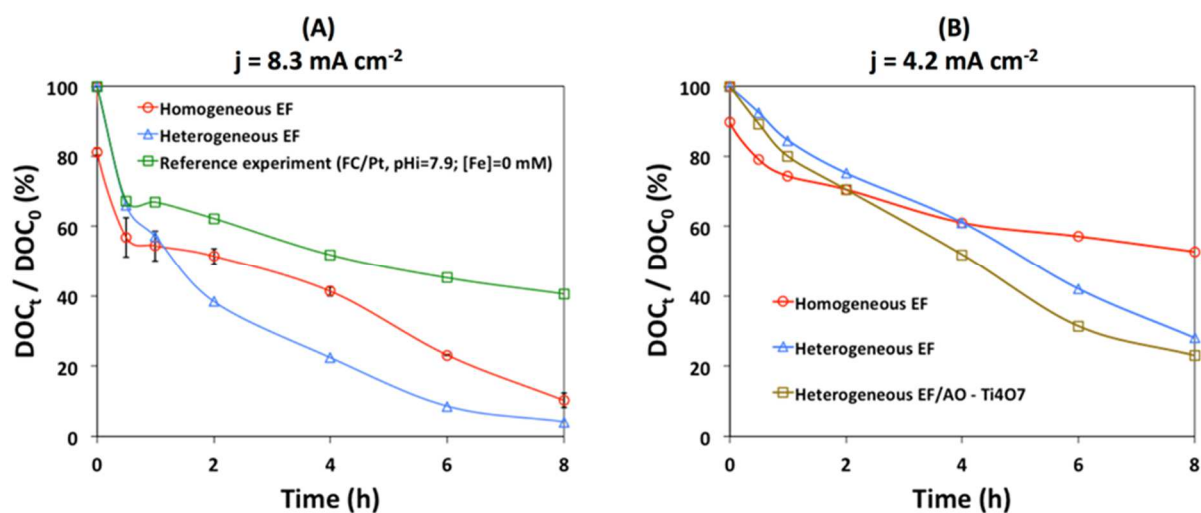
265 Third, experiments were also performed at lower current density ( $4.2 \text{ mA cm}^{-2}$ , Fig. 1B).  
266 Lower DOC removal rates were obtained, e.g. 72% vs 96% removal of DOC after 8 h of  
267 treatment by heterogeneous EF at  $4.2 \text{ mA cm}^{-2}$  and  $8.3 \text{ mA cm}^{-2}$ , respectively. Indeed, high  
268 current density enhances the generation of hydrogen peroxide and regeneration rate of Fe(II).  
269 Thus, further  $\bullet\text{OH}$  are produced for oxidation and mineralization of organic compounds.

270 Fourth, the influence of the anode material was also investigated (Fig. 1B). After 8h of  
271 treatment by heterogeneous EF/AO using  $\text{Ti}_4\text{O}_7$  anode at  $4.2 \text{ mA cm}^{-2}$ , 77% removal of DOC  
272 was achieved, compared to 72% by heterogeneous EF using Pt anode. The higher efficiency  
273 of  $\text{Ti}_4\text{O}_7$  anode was ascribed to the generation at the anode surface of physisorbed  $\text{Ti}_4\text{O}_7(\bullet\text{OH})$   
274 with great oxidation ability, because of the higher overvoltage for oxygen evolution reaction  
275 ( $>0.7 \text{ V}$ ), compared to Pt anode ( $<0.4 \text{ V}$ ) (Trellu et al., 2018a; Ganiyu et al., 2018). Therefore,  
276 by taking also into consideration the lower cost of  $\text{Ti}_4\text{O}_7$ , this anode material appeared as a  
277 suitable electrode to combine AO and EF processes.

278

279





280 **Figure 1** – DOC removal efficiency vs time during the mineralization of NF concentrate.

281 Comparison of different configurations and operating conditions.

282 **(A)  $j = 8.3 \text{ mA cm}^{-2}$**  : (○) Homogeneous EF with CF cathode, Pt anode,  $[\text{Fe}^{2+}] = 0.2 \text{ mmol L}^{-1}$ ,  $\text{pH}_0 = 3$  ; (△) Heterogeneous EF with  $\text{Fe}^{\text{II}}\text{Fe}^{\text{III}}$ -LDH modified CF cathode, Pt anode,  $[\text{Fe}^{2+}] =$   
 283  $0 \text{ mmol L}^{-1}$ ,  $\text{pH}_0 = 7.9$  ; (□) Reference experiment with CF cathode, Pt anode,  $[\text{Fe}^{2+}] = 0 \text{ mmol}$   
 284  $\text{L}^{-1}$ ,  $\text{pH}_0 = 7.9$ . Three homogeneous EF experiments were performed in order to assess the  
 285 reproducibility of the experimental procedure. Standard deviations are reported in Figure 1A.  
 286

287 **(B)  $j = 4.2 \text{ mA cm}^{-2}$**  : (○) Homogeneous EF with CF cathode, Pt anode,  $[\text{Fe}^{2+}] = 0.2 \text{ mmol L}^{-1}$ ,  $\text{pH}_0 = 3$  ; (△) Heterogeneous EF with  $\text{Fe}^{\text{II}}\text{Fe}^{\text{III}}$ -LDH modified CF cathode, Pt anode,  $[\text{Fe}^{2+}] =$   
 288  $0 \text{ mmol L}^{-1}$ ,  $\text{pH}_0 = 7.9$  ; (□) Heterogeneous EF/AO with  $\text{Fe}^{\text{II}}\text{Fe}^{\text{III}}$ -LDH modified CF cathode,  
 289  $\text{Ti}_4\text{O}_7$  anode,  $[\text{Fe}^{2+}] = 0 \text{ mmol L}^{-1}$ ,  $\text{pH}_0 = 7.9$ .  
 290

291

292 One of the main challenges for EAOPs is to reduce the energy consumption (EC). The EC  
 293 was expressed as kWh per g of DOC removed and calculated from Eq. 6 (Brillas et al., 2009).

294

295

296  $EC_{DOC}$  (kWh  $g^{-1}$  of DOC) =  $\frac{E_{cell}It}{V\Delta(DOC)_{exp}}$  (Eq. 6)

297 where  $E_{cell}$  is the average cell voltage (V),  $I$  the applied current (A),  $t$  the duration of  
298 electrolysis (h),  $V$  the volume of solution treated (L) and  $\Delta(DOC)_{exp}$  the experimental decays  
299 of DOC ( $mgC L^{-1}$ ).

300 For example, 96% removal of DOC by heterogeneous EF at  $8.3 mA cm^{-2}$  required 0.35 kWh  
301  $g^{-1}$  of DOC removed. By comparison, 77% DOC removal by heterogeneous EF/AO using  
302  $Ti_4O_7$  anode at  $4.2 mA cm^{-2}$  required only 0.13 kWh  $g^{-1}$  of DOC. This value decreased to 0.11  
303 kWh  $g^{-1}$  of DOC for 45% removal of DOC by the same process (4 h of treatment instead of 8  
304 h). In fact, high current density strongly increased energy consumption because of  
305 concomitant rise in total cell voltage (from 7.2 to 10.4 V). Parasitic reaction such as hydrogen  
306 evolution,  $4 e^{-}$  reduction of  $O_2$  to  $H_2O$  and  $2 e^{-}$  oxidation of water to  $O_2$  are also promoted at  
307 higher current density. Moreover, at high removal rate of DOC and low residual DOC, the  
308 current efficiency is strongly decreased by mass transport limitations. Therefore, in order to  
309 achieve high DOC removal rate with low energy consumption, it was proposed to combine  
310 EAOPs with a biological post-treatment, since EAOPs are able to transform biorefractory  
311 organic compounds into by-products that are more biodegradable than initial compounds  
312 (Ganzenko et al., 2014; Olvera-Vargas et al., 2015; Trellu et al., 2016a). In practice, that  
313 would mean implementing the EAOP as a preliminary treatment before recirculation of the  
314 NF concentrate towards the MBR. Thus, the next objective of this study was to monitor the  
315 evolution of the biodegradability of the effluent, as well as to better understand the evolution  
316 of organic and inorganic compounds during EAOPs.

317

318

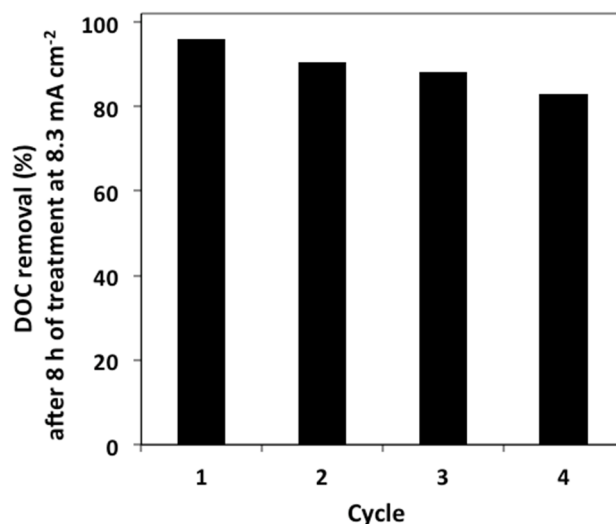


**Figure 2** – DOC removal after 8h of electrolysis vs number of cycles for the heterogeneous EF treatment using Fe<sup>II</sup>Fe<sup>III</sup>-LDH/CF cathode and Pt anode at 8.3 mA cm<sup>-2</sup>.

319

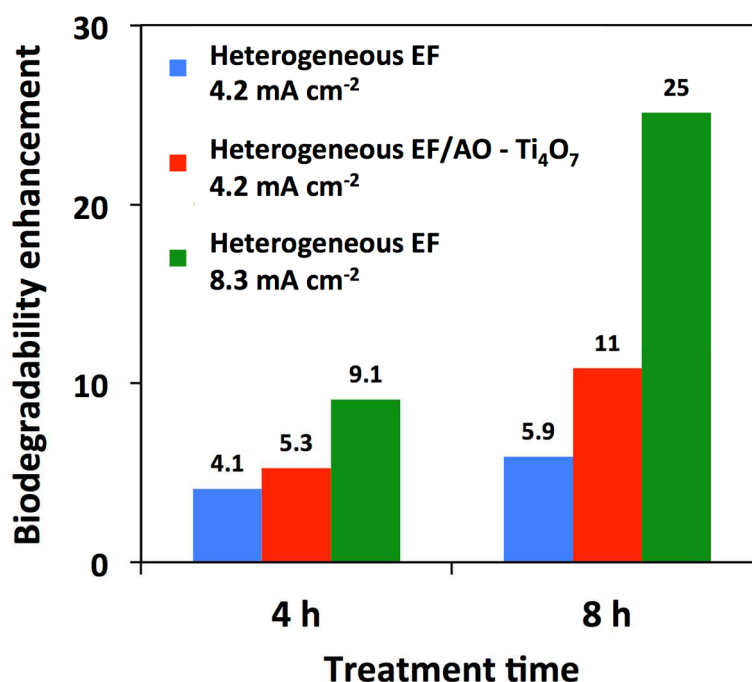
320

### 321 **3.3 Biodegradability enhancement**

322 Respirometric measurements performed have the advantage of being a direct and rapid  
 323 biological assessment of aerobic degradation under similar conditions than in the real  
 324 industrial MBR (Reuschenbach et al., 2003). The calculated biodegradability enhancement  
 325 (BE) values are presented in Fig. 3 after 4 and 8h of treatment for different EAOP  
 326 configurations and current densities applied.

327 In all cases, heterogeneous EF shows an increase in the biodegradability of the NF  
 328 concentrate, which validate the potential positive role of EAOPs as a pre-treatment before  
 329 recirculating the NF concentrate to the MBR. In general the more the mineralization rate is  
 330 achieved the more the biodegradability enhancement is observed. After 8 h of treatment by  
 331 heterogeneous EF at 4.2 mA cm<sup>-2</sup>, the BE index reached 11 with Ti<sub>4</sub>O<sub>7</sub> anode, compared to  
 332 5.9 with Pt anode, which validate the positive effect of combining EF with AO. We could

333 state that a satisfactory biodegradability enhancement (between 4.1 and 9.1) was reached after  
334 4 h with optimal energy consumption efficiency.



335 **Figure 3** – Biodegradability enhancement at two different treatment times for different  
336 EAOPs and current densities.

337

338

### 339 **3.4 Acute toxicity of the effluent**

340 Toxicity evolution of the NF concentrate during its electrolysis by both heterogeneous and  
341 homogeneous EF was evaluated by Microtox<sup>®</sup> standard method (Fig. 4). Initially (i.e. before  
342 any treatment of the NF concentrate), around 50±5% of *V. fischeri* luminescence inhibition  
343 was observed because of the presence of large amount of toxic trace metals and organic  
344 pollutants. *V. fischeri* luminescence inhibition can be sensitive to various phenomena that can  
345 not be controlled and studied separately during the treatment of such complex effluent, e.g.  
346 the removal of toxic organic pollutants, the formation of toxic degradation by-products, the

347 formation of non-toxic degradation by-products (which could promote stimulation of bacterial  
 348 luminescence), the release of inorganic compounds and the evolution of metal speciation.  
 349 Therefore, it is difficult to draw reliable conclusions from these analyses. However, results  
 350 show that EAOPs are not able to remove completely the acute toxicity from such complex  
 351 effluent containing both organic and inorganic toxic compounds. Luminescence inhibition  
 352 might even increase significantly, particularly after achieving high mineralization rates (for  
 353 example during heterogeneous EF at  $8.3 \text{ mA cm}^{-2}$  and heterogeneous EF at  $4.2 \text{ mA cm}^{-2}$ ).  
 354 From the comparison of heterogeneous EF experiments performed with either Pt or  $\text{Ti}_4\text{O}_7$   
 355 anode, it seems that anodic oxidation participate to avoid the accumulation of toxic by-  
 356 products in the bulk.

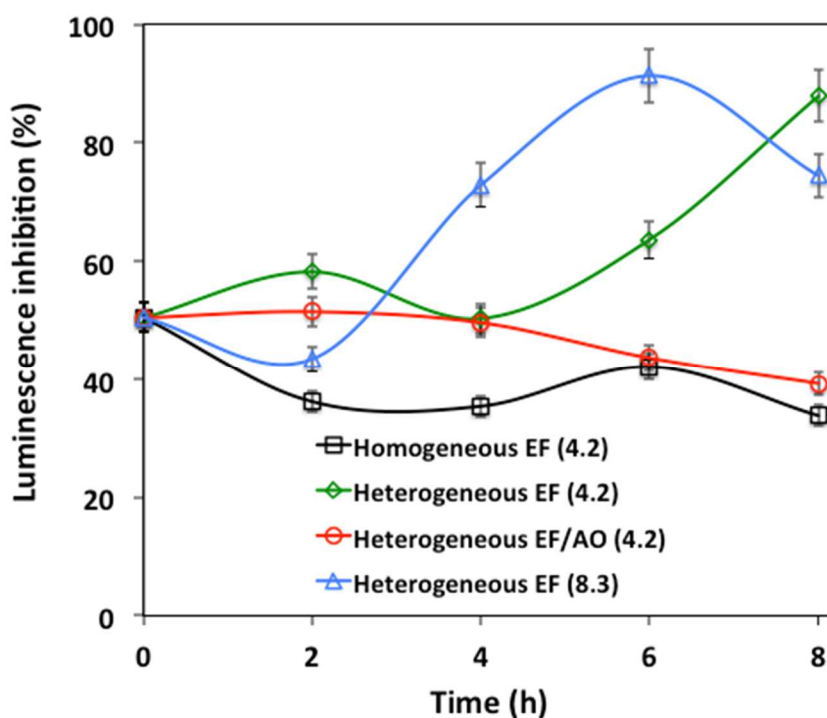


**Figure 4** – Evolution of *Vibrio fischeri* luminescence inhibition (Microtox<sup>®</sup> test) vs electrolysis time according to EAOP configuration and current density (in brackets,  $\text{mA cm}^{-2}$ )

357

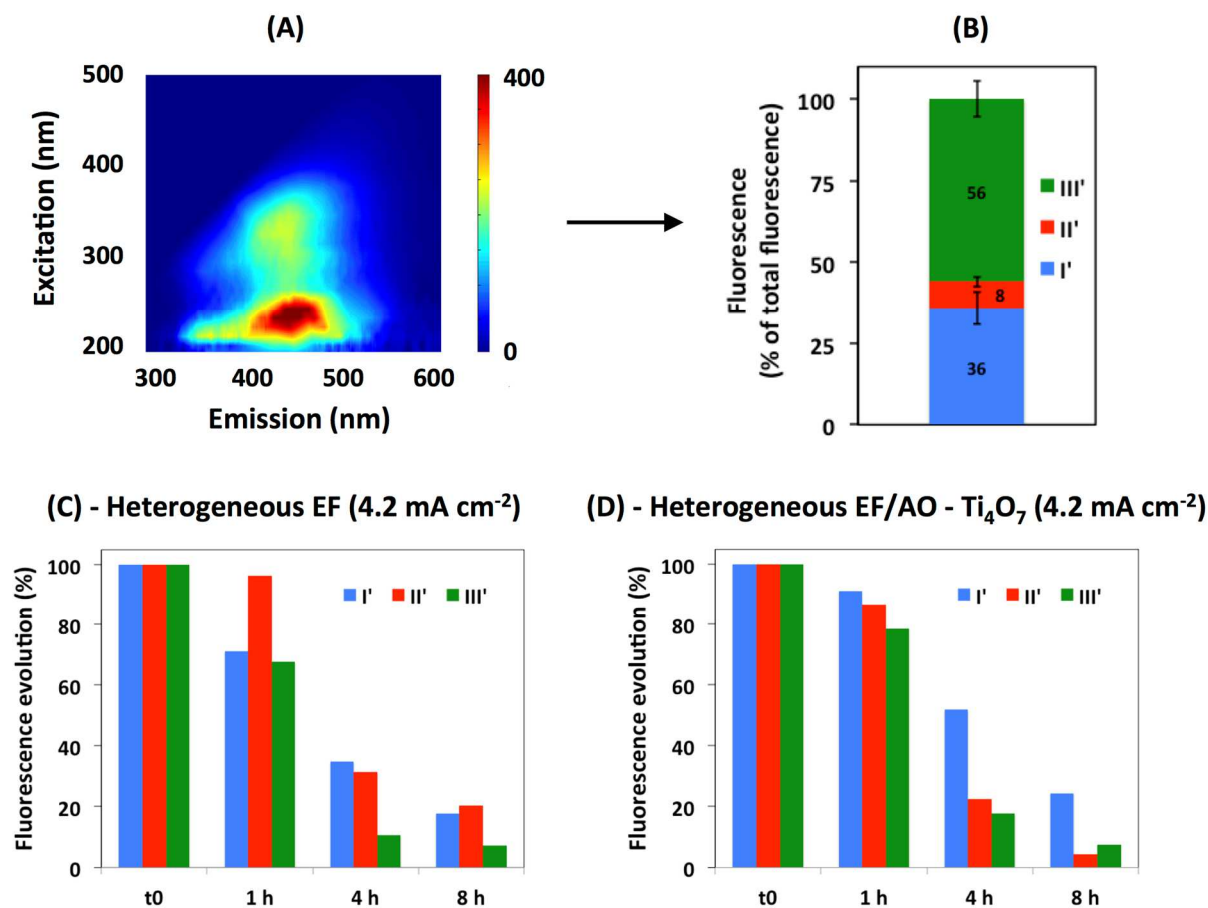
358

### 3.5 Characterization of the organic matter by 3DEEM

3DEEM has been reported to be a useful tool for characterization of colloidal and dissolved organic matter. Particularly, Jacquin et al. (2017) recently emphasized a correlation between the volume of fluorescence of zone III' (HA+FA-like fluorophores) and the concentration in a full-scale MBR of humic substances (MW  $\approx$  1000 Da) and building blocks (degradation by-products from humic substances, with MW  $\approx$  300-500 Da) measured by size exclusion liquid chromatography coupled with organic carbon and organic nitrogen detector. Similarly, a correlation was also obtained between the volume of fluorescence of zone II' (SMP-like fluorophores) and the concentration of proteins from biopolymers (MW  $\approx$  20,000 -  $7.5 \times 10^{11}$  Da). Besides, no correlation was obtained for the volume of fluorescence of zone I' because fluorophores of this zone would be mostly associated with colloidal proteins that could not be analyzed by size exclusion liquid chromatography (Jacquin et al., 2017). In this study, we proposed to use these results with the view to obtain indications on the evolution of the nature of the organic matter during EAOPs.

The initial effluent was mainly constituted of HA+FA-like fluorophores from zone III' as shown in Fig. 5A and 5B. This result is consistent with the pre-treatment of the effluent in the MBR because microfiltration membranes have lower retention capacity for these low MW compounds. A strong decrease of fluorophores of zone III' was then observed during both heterogeneous EF (Fig. 5C) and EF/AO (Fig. 5D) due to (i) precipitation of humic acids at acidic pH and (ii) fast degradation and mineralization of these low MW compounds with an aromatic structure that reacts quickly with  $\cdot\text{OH}$  (Trellu et al., 2016b). By comparison, fluorescence from colloidal proteins of zone I' decreased much more slowly. This phenomenon might be ascribed to the lower availability of colloids for reaction with  $\cdot\text{OH}$  in the aqueous phase. In the context of the global combined process, this result means that improving the retention of colloidal proteins in the MBR would then have a positive effect on

384 the efficiency of the EAOP. Finally, it was also observed that the use of  $Ti_4O_7$  anode for the  
 385 heterogeneous AO/EF process promoted significantly the decrease of the fluorescence of  
 386 proteins from biopolymers (zone II', Fig. 5D). This might be ascribed to the higher electro-  
 387 catalytic activity of  $Ti_4O_7$  for anodic oxidation of organic compounds, compared to Pt anode  
 388 (Ganiyu et al., 2016).



389  
 390 **Figure 5** – Fluorescence evolution of the NF concentrate effluent treated by EAOPs, as a  
 391 function of time treatment. Zone I': colloidal proteins ; zone II': Soluble Microbial by-  
 392 Product (SMP)-like fluorophores ; zone III': Humic and Fulvic acids (HA + FA)-like  
 393 fluorophores.

394

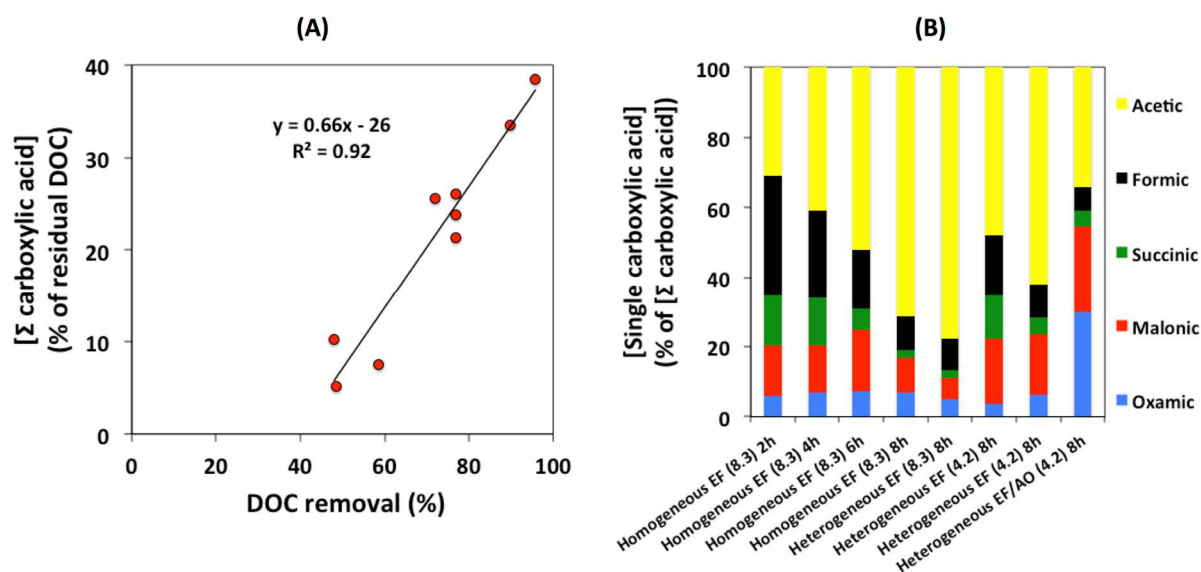
395

### 3.6 Identification and quantification of short-chain carboxylic acids

Short-chain carboxylic acids are common degradation by-products generated during the degradation of organic compounds by EAOPs (Oturán et al., 2008). In this study, they were identified by ion-exclusion HPLC and chromatograms revealed five well defined peaks corresponding to acetic, formic, succinic, malonic and oxamic acids. Results were firstly analyzed by following the evolution of the concentration of the sum of carboxylic acids analyzed. The evolution of the concentration according to treatment time was determined for homogeneous EF at  $8.3 \text{ mA cm}^{-2}$ . An initial increase of the concentration was observed until  $t = 6 \text{ h}$  ( $[\Sigma \text{ carboxylic acids}] = 55 \text{ mgC L}^{-1}$ ) because of the degradation of aromatic pollutants. Then, the concentration decreased ( $[\Sigma \text{ carboxylic acids}] = 34 \text{ mgC L}^{-1}$  at  $t = 8 \text{ h}$ ). In fact, the lower concentration of organic compounds after 6 hours of treatment resulted in lower formation rate of carboxylic acids compared to the degradation rate. Interestingly, Fig. 6A shows a linear correlation ( $R^2 = 0.92$ ) between DOC removal (%) and proportion of carboxylic acids among the residual DOC. This correlation took into consideration all analyzes performed for the different configurations tested. The higher the DOC removal achieved, the higher was the proportion of carboxylic acids among the residual DOC. This result is consistent with the lower reaction rate constant of short-chain carboxylic acids with  $\bullet\text{OH}$  ( $10^7 - 10^8 \text{ M}^{-1} \text{ s}^{-1}$ ) compared to aromatic compounds ( $10^9 - 10^{10} \text{ M}^{-1} \text{ s}^{-1}$ ) from which they are formed (Oturán et al., 2008). The evolution of the proportion of each single carboxylic acid was also studied (Fig. 6B). It was noticed that the proportion of acetic acid among total carboxylic acid concentration was continuously increased over time during homogeneous EF at  $8.3 \text{ mA cm}^{-2}$ . This phenomenon is also consistent with the lower reaction rate constant of acetic acid with  $\bullet\text{OH}$  ( $1.6 \times 10^7 \text{ M}^{-1} \text{ s}^{-1}$ ) compared to other carboxylic acids (Oturán et al., 2008). Similar trend was observed after 8 h of electrolysis using heterogeneous EF at  $8.3 \text{ mA cm}^{-2}$  or  $4.2 \text{ mA cm}^{-2}$  and homogeneous EF at  $4.2 \text{ mA cm}^{-2}$ , i.e. the higher the DOC removal



421 rate (Fig. 1), the higher the proportion of acetic acid. Heterogeneous EF/AO using  $Ti_4O_7$  was  
 422 the only experiment exhibiting a different trend, thus indicating that  $Ti_4O_7$  might modify  
 423 mineralization mechanisms, compared to Pt anode. Higher proportion of N-containing oxamic  
 424 acid and lower proportion of acetic acid were observed with  $Ti_4O_7$  anode, which might be  
 425 attributed to the better electro-catalytic ability of  $Ti_4O_7$  anode for the degradation of organic  
 426 nitrogen and acetic acid, compared to Pt anode. As regards to oxamic acid, these results were  
 427 consistent with 3DEEM. In fact,  $Ti_4O_7$  anode further degraded proteins from biopolymers  
 428 (zone II'), which usually contain high concentration of N (ratio C/N around 3) (Jacquin et al.,  
 429 2017). Overall, the increase of the proportion of carboxylic acids over time confirms the  
 430 suitability of the combination of EAOPs with a biological treatment (Fig. 3), because of the  
 431 well-known high biodegradability of such compounds.



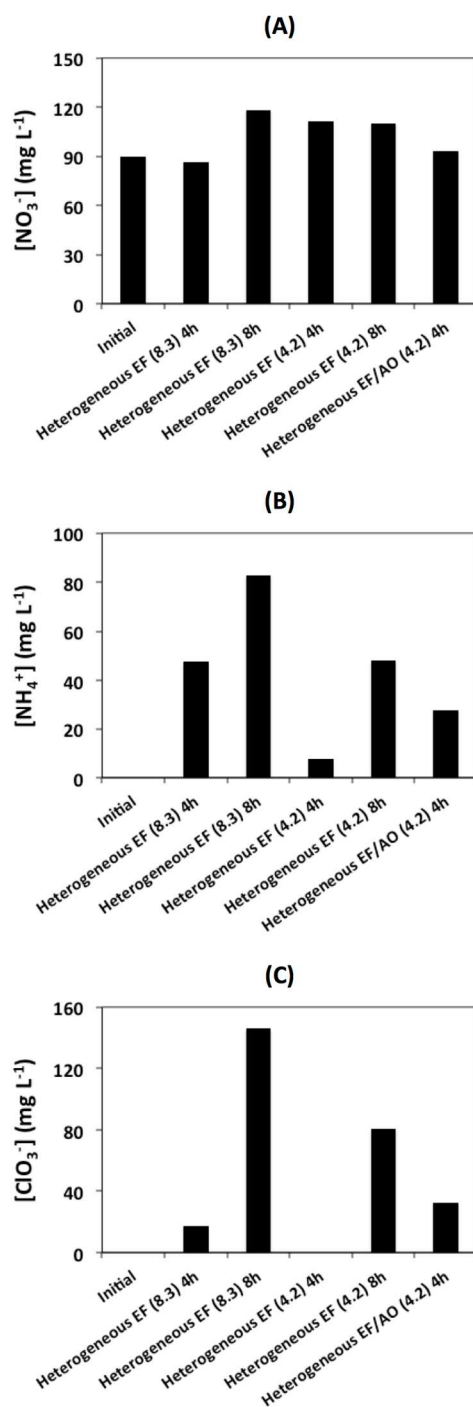
432  
 433 **Figure 6** – Generation of short-chain carboxylic acids during EAOPs: (A) correlation  
 434 between DOC removal (%) and proportion of carboxylic acids among the residual DOC;  
 435 (B) evolution of the proportion of each single carboxylic acid among the total carboxylic acid  
 436 concentration as a function of configurations and operating conditions (current density in  
 437 bracket,  $mA\ cm^{-2}$ ).

### 438 3.7 Evolution of inorganic species

439 Mineralization of  $\text{Cl}^-$  and N-containing organic compounds was accompanied by the  
440 formation of inorganic ions. The main inorganic species of interest ( $\text{NO}_3^-$ ,  $\text{NH}_4^+$ ,  $\text{ClO}_3^-$  and  
441  $\text{ClO}_4^-$ ) were analyzed by ion chromatography. Results are presented in Fig. 7. In all  
442 experiments, a stronger increase of the concentration of  $\text{NH}_4^+$  was observed compared to  $\text{NO}_3^-$   
443 (Fig. 7A and 7B). These results can be explained by (i) the direct release of  $\text{NH}_4^+$  from  
444 mineralization of organic nitrogen and (ii) the release of  $\text{NO}_3^-$  followed by reduction of  $\text{NO}_3^-$   
445 into  $\text{NH}_4^+$  at the cathode. Actually, the latter reaction is often observed during EF and AO,  
446 while oxidation of  $\text{NH}_4^+$  at the anode is hindered by the positive charge of this ion (Martin de  
447 Vidales et al., 2016; Mousset et al., 2018). The amount of  $\text{NH}_4^+$  in the solution increased with  
448 treatment time and current density because of the higher mineralization rate of organic  
449 nitrogen (Fig. 7B). Higher concentration of  $\text{NH}_4^+$  was also obtained using  $\text{Ti}_4\text{O}_7$  anode  
450 (heterogeneous EF/AO), compared to Pt anode (heterogeneous EF). This phenomenon is  
451 consistent with the results obtained from 3DEEM and with the higher concentration of  
452 oxamic acid previously reported, and supports the higher electro-catalytic activity of  $\text{Ti}_4\text{O}_7$  for  
453 the degradation of organic nitrogen. In the context of a treatment strategy including a  
454 recirculation of the effluent back to the MBR, the release of  $\text{NH}_4^+$  during EAOPs would  
455 require further biological nitrification in the MBR.

456 Oxidation of  $\text{Cl}^-$  resulted in a strong increase of  $\text{ClO}_3^-$  concentration (Fig. 7C). The reaction  
457 mechanisms usually go through  $\text{Cl}^-$  oxidation into  $\text{Cl}_2$ , followed by hydrolysis of  $\text{Cl}_2$  into  
458 hypochlorous acid  $\text{HOCl}$ . Further oxidation of  $\text{HOCl}$  lead to the formation of  $\text{ClO}_2^-$  (which  
459 was not detected because of the fast oxidation kinetic) and subsequently  $\text{ClO}_3^-$ . No formation  
460 of  $\text{ClO}_4^-$  was detected in any experiment because higher current density ( $> 30 \text{ mA cm}^{-2}$ ) is  
461 required to form this compound (Mousset et al., 2018). Besides, it was also observed that the  
462 formation of  $\text{ClO}_3^-$  mainly occurred between 4 and 8 h of treatment, most probably because of

463 the preferential reaction of HOCl with organic species and  $\text{NH}_4^+$  (break-point chlorination)  
464 between 4 and 8 h of treatment (Martin de Vidales et al., 2016; Mousset et al., 2018). These  
465 results confirm the suitability to stop the treatment after 4 h of treatment in order to avoid the  
466 accumulation of  $\text{ClO}_3^-$  and  $\text{NH}_4^+$ . While  $\text{ClO}_3^-$  can be toxic for the biomass in the MBR, the  
467 formation of  $\text{NH}_3$  at basic pH is also highly toxic for the autotrophic biomass (Jacquin et al.,  
468 2018).



469 **Figure 7** – Concentration evolution of main inorganic species of interest during EAOPs as a  
 470 function of configurations and operating conditions (current density in bracket, mA cm<sup>-2</sup>): (A)  
 471 ClO<sub>3</sub><sup>-</sup>, (B) NO<sub>3</sub><sup>-</sup> and (C) NH<sub>4</sub><sup>+</sup>. ClO<sub>4</sub><sup>-</sup> was not detected.

472

473

## 474 **4. Conclusion**

475 NF concentrate of landfill leachate pre-treated in a MBR contains high concentration of  
476 biorefractory organic pollutants that makes very difficult to treat or detoxify by conventional  
477 techniques. The investigation of different configurations of EAOPs applied to this complex  
478 effluent showed that heterogeneous EF/AO using  $\text{Ti}_4\text{O}_7$  anode and  $\text{Fe}^{\text{II}}\text{Fe}^{\text{III}}$ -LDH modified CF  
479 cathode is the most efficient process for mineralization of organic pollutants. Without initial  
480 pH adjustment and external addition of  $\text{Fe}^{2+}$  in the bulk, 45% removal of DOC was achieved  
481 at  $4.2 \text{ mA cm}^{-2}$  with limited energy consumption ( $0.11 \text{ kWh g}^{-1}$  of DOC removed, i.e.  $49.5$   
482  $\text{ kWh m}^{-3}$ ). Up to 96% removal of DOC was also obtained by using higher current density ( $8.3$   
483  $\text{ mA cm}^{-2}$ ) during the heterogeneous EF process. The use of  $\text{Ti}_4\text{O}_7$  anode appeared to be a key  
484 parameter for improving the degradation and mineralization of organic nitrogen. From  
485 3DEEM analysis, colloidal proteins were observed to be the most refractory organic  
486 compounds. Therefore, improving the retention of such compounds in the MBR could  
487 improve the efficiency of the EAOP.

488 The acute toxicity of the effluent was not removed but strong biodegradability enhancement  
489 was observed after 4 h of treatment by heterogeneous EF/AO, thus making possible the  
490 recirculation of the residual DOC towards the MBR in order to achieve total COD removal  
491 without longer electrochemical treatment time. This result was consistent with the  
492 identification and quantification of more biodegradable and less toxic by-products such as  
493 carboxylic acids. In fact, a linear correlation was observed between DOC removal rate and  
494 proportion of carboxylic acids in the residual DOC. As regards to the fate of inorganic  
495 species, the formation of  $\text{ClO}_3^-$  could be limited by stopping electro-oxidation at 4 h, but  
496 enhanced nitrification would be required in the MBR because of the release of  $\text{NH}_4^+$  from  
497 mineralization of organic nitrogen. Overall, these results emphasized the interdependence

498 between the MBR process and the EAOP in a combined treatment strategy and demonstrated  
499 that the use of EAOPs using suitable electrode materials can be useful for the management of  
500 such complex effluent.

## 501 **Acknowledgements**

502 We gratefully acknowledge the National French Agency of Research ‘ANR’ for funding the  
503 project ECOTS/CELECTRON. Authors are also grateful to Saint Gobain Research Provence  
504 for supplying  $Ti_4O_7$  electrodes.

505

506

507

508

509

510

511

512

513

514

## 515 **References**

- 516 Amaral, M.C., Moravia, W.G., Lange, L.C., Zico, M.R., Magalhães, N.C., Ricci, B.C., Reis, B.G.,  
517 2016. Pilot aerobic membrane bioreactor and nanofiltration for municipal landfill leachate  
518 treatment. *Journal of Environmental Science and Health, Part A* 51, 640–649.
- 519 Ammar, S., Oturan, M.A., Labiadh, L., Guersalli, A., Abdelhedi, R., Oturan, N., Brillas, E., 2015.  
520 Degradation of tyrosol by a novel electro-Fenton process using pyrite as heterogeneous  
521 source of iron catalyst. *Water Research* 74, 77–87.  
522 <https://doi.org/10.1016/j.watres.2015.02.006>
- 523 Brillas, E., Sirés, I., Oturan, M.A., 2009. Electro-Fenton Process and Related Electrochemical  
524 Technologies Based on Fenton's Reaction Chemistry. *Chemical Reviews* 109, 6570–6631.  
525 <https://doi.org/10.1021/cr900136g>
- 526 Campagna, M., Çakmakçı, M., Büşra Yaman, F., Özkaya, B., 2013. Molecular weight  
527 distribution of a full-scale landfill leachate treatment by membrane bioreactor and  
528 nanofiltration membrane. *Waste Management* 33, 866–870.  
529 <https://doi.org/10.1016/j.wasman.2012.12.010>
- 530 Chen, W., Westerhoff, P., Leenheer, J.A., Booksh, K., 2003. Fluorescence Excitation–Emission  
531 Matrix Regional Integration to Quantify Spectra for Dissolved Organic Matter. *Environmental*  
532 *Science & Technology* 37, 5701–5710. <https://doi.org/10.1021/es034354c>
- 533 Comninellis, C., Kapalka, A., Malato, S., Parsons, S.A., Poulios, I., Mantzavinos, D., 2008.  
534 Advanced oxidation processes for water treatment: Advances and trends for R&D. *J. Chem.*  
535 *Technol. Biotechnol.* 83, 769–776. <https://doi.org/10.1002/jctb.1873>
- 536 Cui, Y.-H., Xue, W.-J., Yang, S.-Q., Tu, J.-L., Guo, X.-L., Liu, Z.-Q., 2018.  
537 Electrochemical/peroxydisulfate/Fe<sup>3+</sup> treatment of landfill leachate nanofiltration  
538 concentrate after ultrafiltration. *Chemical Engineering Journal* 353, 208–217.  
539 <https://doi.org/10.1016/j.cej.2018.07.101>
- 540 Ganiyu, S.O., Huong Le, T.X., Bechelany, M., Oturan, N., Papirio, S., Esposito, G., van  
541 Hullebusch, E., Cretin, M., Oturan, M.A., 2018. Electrochemical mineralization of  
542 sulfamethoxazole over wide pH range using FeII/FeIII LDH modified carbon felt cathode:  
543 Degradation pathway, toxicity and reusability of the modified cathode. *Chemical Engineering*  
544 *Journal* 350, 844–855. <https://doi.org/10.1016/j.cej.2018.04.141>
- 545 Ganiyu, S.O., Le, T.X.H., Bechelany, M., Esposito, G., Hullebusch, E.D. van, Oturan, M.A.,  
546 Cretin, M., 2017a. A hierarchical CoFe-layered double hydroxide modified carbon-felt  
547 cathode for heterogeneous electro-Fenton process. *J. Mater. Chem. A* 5, 3655–3666.  
548 <https://doi.org/10.1039/C6TA09100H>
- 549 Ganiyu, S.O., Oturan, N., Raffy, S., Cretin, M., Esmilaire, R., van Hullebusch, E., Esposito, G.,  
550 Oturan, M.A., 2016. Sub-stoichiometric titanium oxide (Ti<sub>4</sub>O<sub>7</sub>) as a suitable ceramic anode  
551 for electrooxidation of organic pollutants: A case study of kinetics, mineralization and

552 toxicity assessment of amoxicillin. *Water Research* 106, 171–182.  
553 <https://doi.org/10.1016/j.watres.2016.09.056>

554 Ganiyu, S.O., Oturan, N., Raffy, S., Esposito, G., van Hullebusch, E.D., Cretin, M., Oturan,  
555 M.A., 2017b. Use of Sub-stoichiometric Titanium Oxide as a Ceramic Electrode in Anodic  
556 Oxidation and Electro-Fenton Degradation of the Beta-blocker Propranolol: Degradation  
557 Kinetics and Mineralization Pathway. *Electrochimica Acta* 242, 344–354.  
558 <https://doi.org/10.1016/j.electacta.2017.05.047>

559 Ganiyu, S. O., Zhou, M., Martínez-Huitle, C. A., 2018. Heterogeneous electro-Fenton and  
560 photoelectro-Fenton processes: a critical review of fundamental principles and application  
561 for water/wastewater treatment. *Applied Catalysis B: Environmental* 235, 103-129.  
562 <https://doi.org/10.1016/j.apcatb.2018.04.044>

563 Ganzenko, O., Huguenot, D., van Hullebusch, E.D., Esposito, G., Oturan, M.A., 2014.  
564 Electrochemical advanced oxidation and biological processes for wastewater treatment: a  
565 review of the combined approaches. *Environmental Science and Pollution Research* 21,  
566 8493–8524. <https://doi.org/10.1007/s11356-014-2770-6>

567 Ganzenko, O., Trelu, C., Papirio, S., Oturan, N., Huguenot, D., van Hullebusch, E.D., Esposito,  
568 G., Oturan, M.A., 2018. Bioelectro-Fenton: evaluation of a combined biological—advanced  
569 oxidation treatment for pharmaceutical wastewater. *Environmental Science and Pollution*  
570 *Research* 25, 20283–20292. <https://doi.org/10.1007/s11356-017-8450-6>

571 García-Rodríguez, O., Bañuelos, J.A., El-Ghenymy, A., Godínez, L.A., Brillas, E., Rodríguez-  
572 Valadez, F.J., 2016. Use of a carbon felt–iron oxide air-diffusion cathode for the  
573 mineralization of Malachite Green dye by heterogeneous electro-Fenton and UVA  
574 photoelectro-Fenton processes. *Journal of Electroanalytical Chemistry* 767, 40–48.  
575 <https://doi.org/10.1016/j.jelechem.2016.01.035>

576 Guo, L., Jing, Y., Chaplin, B.P., 2016. Development and Characterization of Ultrafiltration TiO<sub>2</sub>  
577 Magnéli Phase Reactive Electrochemical Membranes. *Environ. Sci. Technol.* 50, 1428–1436.  
578 <https://doi.org/10.1021/acs.est.5b04366>

579 Hu, Y., Lu, Y., Liu, G., Luo, H., Zhang, R., Cai, X., 2018. Effect of the structure of stacked  
580 electro-Fenton reactor on treating nanofiltration concentrate of landfill leachate.  
581 *Chemosphere* 202, 191–197. <https://doi.org/10.1016/j.chemosphere.2018.03.103>

582 Iglesias, O., Fernández de Dios, M.A., Pazos, M., Sanromán, M.A., 2013. Using iron-loaded  
583 sepiolite obtained by adsorption as a catalyst in the electro-Fenton oxidation of Reactive  
584 Black 5. *Environmental Science and Pollution Research* 20, 5983–5993.  
585 <https://doi.org/10.1007/s11356-013-1610-4>

586 Jacquin, C., Lesage, G., Traber, J., Pronk, W., Heran, M., 2017. Three-dimensional excitation  
587 and emission matrix fluorescence (3DEEM) for quick and pseudo-quantitative determination  
588 of protein- and humic-like substances in full-scale membrane bioreactor (MBR). *Water*  
589 *Research* 118, 82–92. <https://doi.org/10.1016/j.watres.2017.04.009>

590 Jacquin, C., Monnot, M., Hamza, R., Kouadio, Y., Zaviska, F., Merle, T., Lesage, G., Héran, M.,



591 2018. Link between dissolved organic matter transformation and process performance in a  
592 membrane bioreactor for urinary nitrogen stabilization. *Environmental Science: Water*  
593 *Research & Technology* 4, 806–819. <https://doi.org/10.1039/C8EW00029H>

594 Kjeldsen, P., Barlaz, M.A., Rooker, A.P., Baun, A., Ledin, A., Christensen, T.H., 2002. Present  
595 and Long-Term Composition of MSW Landfill Leachate: A Review. *Critical Reviews in*  
596 *Environmental Science and Technology* 32, 297–336.  
597 <https://doi.org/10.1080/10643380290813462>

598 Li, X., Zhu, W., Wu, Y., Wang, C., Zheng, J., Xu, K., Li, J., 2015. Recovery of potassium from  
599 landfill leachate concentrates using a combination of cation-exchange membrane  
600 electrolysis and magnesium potassium phosphate crystallization. *Separation and Purification*  
601 *Technology* 144, 1–7. <https://doi.org/10.1016/j.seppur.2015.01.035>

602 Ma, L., Zhou, M., Ren, G., Yang, W., Liang, L., 2016. A highly energy-efficient flow-through  
603 electro-Fenton process for organic pollutants degradation. *Electrochimica Acta* 200, 222–  
604 230. <https://doi.org/10.1016/j.electacta.2016.03.181>

605 Mahindrakar, K.V., Rathod, V.K., 2018. Utilization of banana peels for removal of strontium  
606 (II) from water. *Environmental Technology & Innovation* 11, 371–383.  
607 <https://doi.org/10.1016/j.eti.2018.06.015>

608 Martín de Vidales, M.J., Millán, M., Sáez, C., Cañizares, P., Rodrigo, M.A., 2016. What  
609 happens to inorganic nitrogen species during conductive diamond electrochemical oxidation  
610 of real wastewater? *Electrochemistry Communications* 67, 65–68.  
611 <https://doi.org/10.1016/j.elecom.2016.03.014>

612 Martínez-Huitle, C.A., Rodrigo, M.A., Sirés, I., Scialdone, O., 2015. Single and Coupled  
613 Electrochemical Processes and Reactors for the Abatement of Organic Water Pollutants: A  
614 Critical Review. *Chem. Rev.* 115, 13362–13407.  
615 <https://doi.org/10.1021/acs.chemrev.5b00361>

616 Mousset, E., Pontvianne, S., Pons, M.-N., 2018. Fate of inorganic nitrogen species under  
617 homogeneous Fenton combined with electro-oxidation/reduction treatments in synthetic  
618 solutions and reclaimed municipal wastewater. *Chemosphere* 201, 6–12.  
619 <https://doi.org/10.1016/j.chemosphere.2018.02.142>

620 Oller, I., Malato, S., Sánchez-Pérez, J.A., 2011. Combination of Advanced Oxidation Processes  
621 and biological treatments for wastewater decontamination—A review. *Science of The Total*  
622 *Environment* 409, 4141–4166. <https://doi.org/10.1016/j.scitotenv.2010.08.061>

623 Olvera-Vargas, H., Cocerva, T., Oturan, N., Buisson, D., Oturan, M.A., 2015. Bioelectro-  
624 Fenton: A sustainable integrated process for removal of organic pollutants from water:  
625 Application to mineralization of metoprolol. *J. Hazard. Mater.*  
626 <https://doi.org/10.1016/j.jhazmat.2015.12.010>

627 Oturan, M.A., Pimentel, M., Oturan, N., Sirés, I., 2008. Reaction sequence for the  
628 mineralization of the short-chain carboxylic acids usually formed upon cleavage of aromatics  
629 during electrochemical Fenton treatment. *Electrochimica Acta* 54, 173–182.

630 <https://doi.org/10.1016/j.electacta.2008.08.012>

631 Oturan, N., van Hullebusch, E.D., Zhang, H., Mazeas, L., Budzinski, H., Le Menach, K., Oturan,  
632 M.A., 2015. Occurrence and Removal of Organic Micropollutants in Landfill Leachates  
633 Treated by Electrochemical Advanced Oxidation Processes. *Environmental Science &*  
634 *Technology* 49, 12187–12196. <https://doi.org/10.1021/acs.est.5b02809>

635 Özcan, A., Sahin, Y., Koparal, A.S., Oturan, M.A., 2008. Prophan mineralization in aqueous  
636 medium by anodic oxidation using boron-doped diamond anode: Influence of experimental  
637 parameters on degradation kinetics and mineralization efficiency. *Water Res.* 42, 2889–  
638 2898. <https://doi.org/10.1016/j.watres.2008.02.027>

639 Panizza, M., Cerisola, G., 2009. Direct and mediated anodic oxidation of organic pollutants.  
640 *Chem. Rev.* 109, 6541–6569. <https://doi.org/10.1021/cr9001319>

641 Ponthieu, M., Pinel-Raffaitin, P., Le Hecho, I., Mazeas, L., Amouroux, D., Donard, O.F.X.,  
642 Potin-Gautier, M., 2007. Speciation analysis of arsenic in landfill leachate. *Water Research*  
643 41, 3177–3185. <https://doi.org/10.1016/j.watres.2007.04.026>

644 Poza-Nogueiras, V., Rosales, E., Pazos, M., Sanromán, M. Á. (2018). Current advances and  
645 trends in electro-Fenton process using heterogeneous catalysts—a review. *Chemosphere* 201,  
646 399-416. <https://doi.org/10.1016/j.chemosphere.2018.03.002>

647 Radjenovic, J., Sedlak, D.L., 2015. Challenges and Opportunities for Electrochemical  
648 Processes as Next-Generation Technologies for the Treatment of Contaminated Water.  
649 *Environ. Sci. Technol.* 49, 11292–11302. <https://doi.org/10.1021/acs.est.5b02414>

650 Reuschenbach, P., Pagga, U., Strotmann, U., 2003. A critical comparison of respirometric  
651 biodegradation tests based on OECD 301 and related test methods. *Water Research* 37,  
652 1571–1582. [https://doi.org/10.1016/S0043-1354\(02\)00528-6](https://doi.org/10.1016/S0043-1354(02)00528-6)

653 Sirés, I., Brillas, E., Oturan, M.A., Rodrigo, M.A., Panizza, M., 2014. Electrochemical advanced  
654 oxidation processes: today and tomorrow. A review. *Environ Sci Pollut Res* 21, 8336–8367.  
655 <https://doi.org/10.1007/s11356-014-2783-1>

656 Trellu, C., Chaplin, B.P., Coetsier, C., Esmilaire, R., Cerneaux, S., Causserand, C., Cretin, M.,  
657 2018a. Electro-oxidation of organic pollutants by reactive electrochemical membranes.  
658 *Chemosphere* 208, 159–175. <https://doi.org/10.1016/j.chemosphere.2018.05.026>

659 Trellu, C., Coetsier, C., Rouch, J.-C., Esmilaire, R., Rivallin, M., Cretin, M., Causserand, C.,  
660 2018b. Mineralization of organic pollutants by anodic oxidation using reactive  
661 electrochemical membrane synthesized from carbothermal reduction of TiO<sub>2</sub>. *Water*  
662 *Research* 131, 310–319. <https://doi.org/10.1016/j.watres.2017.12.070>

663 Trellu, C., Ganzenko, O., Papirio, S., Pechaud, Y., Oturan, N., Huguenot, D., van Hullebusch,  
664 E.D., Esposito, G., Oturan, M.A., 2016a. Combination of anodic oxidation and biological  
665 treatment for the removal of phenanthrene and Tween 80 from soil washing solution.  
666 *Chemical Engineering Journal* 306, 588–596. <https://doi.org/10.1016/j.cej.2016.07.108>

667 Trellu, C., Oturan, N., Pechaud, Y., van Hullebusch, E.D., Esposito, G., Oturan, M.A., 2017.

668 Anodic oxidation of surfactants and organic compounds entrapped in micelles – Selective  
669 degradation mechanisms and soil washing solution reuse. *Water Research* 118, 1–11.  
670 <https://doi.org/10.1016/j.watres.2017.04.013>

671 Trellu, C., Péchaud, Y., Oturan, N., Mousset, E., Huguenot, D., van Hullebusch, E.D., Esposito,  
672 G., Oturan, M.A., 2016b. Comparative study on the removal of humic acids from drinking  
673 water by anodic oxidation and electro-Fenton processes: Mineralization efficiency and  
674 modelling. *Applied Catalysis B: Environmental* 194, 32–41.  
675 <https://doi.org/10.1016/j.apcatb.2016.04.039>

676 Van der Bruggen, B., Koninckx, A., Vandecasteele, C., 2004. Separation of monovalent and  
677 divalent ions from aqueous solution by electrodialysis and nanofiltration. *Water Research*  
678 38, 1347–1353. <https://doi.org/10.1016/j.watres.2003.11.008>

679 Van der Bruggen, B., Lejon, L., Vandecasteele, C., 2003. Reuse, Treatment, and Discharge of  
680 the Concentrate of Pressure-Driven Membrane Processes. *Environmental Science &*  
681 *Technology* 37, 3733–3738. <https://doi.org/10.1021/es0201754>

682 Wang, Yujing, Zhao, G., Chai, S., Zhao, H., Wang, Yanbin, 2013. Three-Dimensional  
683 Homogeneous Ferrite-Carbon Aerogel: One Pot Fabrication and Enhanced Electro-Fenton  
684 Reactivity. *ACS Applied Materials & Interfaces* 5, 842–852.  
685 <https://doi.org/10.1021/am302437a>

686 Westerhoff, P., Prapaipong, P., Shock, E., Hillaireau, A., 2008. Antimony leaching from  
687 polyethylene terephthalate (PET) plastic used for bottled drinking water. *Water Research* 42,  
688 551–556. <https://doi.org/10.1016/j.watres.2007.07.048>

689 Xu, Y., Chen, C., Li, X., Lin, J., Liao, Y., Jin, Z., 2017. Recovery of humic substances from  
690 leachate nanofiltration concentrate by a two-stage process of tight ultrafiltration membrane.  
691 *Journal of Cleaner Production* 161, 84–94. <https://doi.org/10.1016/j.jclepro.2017.05.095>

692 Zhang, G., Wang, S., Yang, F., 2012. Efficient Adsorption and Combined  
693 Heterogeneous/Homogeneous Fenton Oxidation of Amaranth Using Supported Nano-FeOOH  
694 As Cathodic Catalysts. *The Journal of Physical Chemistry C* 116, 3623–3634.  
695 <https://doi.org/10.1021/jp210167b>

696 Zhang, H., Fei, C., Zhang, D., Tang, F., 2007. Degradation of 4-nitrophenol in aqueous  
697 medium by electro-Fenton method. *Journal of Hazardous Materials* 145, 227–232.  
698 <https://doi.org/10.1016/j.jhazmat.2006.11.016>

699 Zhang, L., Li, A., Lu, Y., Yan, L., Zhong, S., Deng, C., 2009. Characterization and removal of  
700 dissolved organic matter (DOM) from landfill leachate rejected by nanofiltration. *Waste*  
701 *Management* 29, 1035–1040. <https://doi.org/10.1016/j.wasman.2008.08.020>

702 Zhang, Q.-Q., Tian, B.-H., Zhang, X., Ghulam, A., Fang, C.-R., He, R., 2013. Investigation on  
703 characteristics of leachate and concentrated leachate in three landfill leachate treatment  
704 plants. *Waste Management* 33, 2277–2286. <https://doi.org/10.1016/j.wasman.2013.07.021>